Structural Engineering and Mechanics, *Vol. 61, No. 5 (2017) 675-684*
DOI: https://doi.org/10.12989/sem.2017.61.5.675

A hybrid seismic response control to improve performance of a two-span bridge

Gwanghee Heo[1a], Chunggil Kim[*1], Seunggon Jeon[2b], Chinok Lee[2a] and Joonryong Jeon[1c]

[1]*Department of Civil Engineering, Konyang University, 121 Daehak-ro, Nonan, Chungcheongnam 32992, Republic of Korea*
[2]*Department of Civil Engineering, Chungnam National University, 99 Daehak-ro, Yuseong-gu, Daejeon 34134, Republic of Korea*

(Received December 4, 2015, Revised December 29, 2016, Accepted January 25, 2017)

Abstract. In this paper, a hybrid seismic response control (HSRC) system was developed to control bridge behavior caused by the seismic load. It was aimed at optimum vibration control, composed of a rubber bearing of passive type and MR-damper of semi-active type. Its mathematical modeling was driven and applied to a bridge model so as to prove its validity. The bridge model was built for the experiment, a two-span bridge of 8.3 meters in length with the HSRC system put up on it. Then, inflicting the EI Centro seismic load on it, shaking table tests were carried out to confirm the system's validity. The experiments were conducted under the basic structure state (without an MR-damper applied) first, and then under the state with an MR-damper applied. It was also done under the basic structure state with a reinforced rubber bearing applied, then the passive on/off state of the HSRC system, and finally the semi-active state where the control algorithm was applied to the system. From the experiments, it was observed that pounding rather increased when the MR-damper alone was applied, and also that the application of the HSRC system effectively prevented it from occurring. That is, the experiments showed that the system successfully mitigated structural behavior by 70% against the basic structure state, and, further, when control algorithm is applied for the operation of the MR-damper, relative displacement was found to be effectively mitigated by 80%. As a result, the HSRC system was proven to be effective in mitigating responses of the two-span bridge under seismic load.

Keywords: hybrid seismic response control system; rubber bearing; MR-damper; shaking table test; control algorithm

1. Introduction

When an earthquake occurs thus affecting bridges, there may be pounding between their upper structure and abutment, and also between upper structures themselves, causing serious damage on them. Two of the most outstanding cases of damage are found in the Loma Prieta (1989) and Kobe (1995) earthquake, where disparate movement of each upper span caused a destruction of whole bridges (Zanardo 2002). Besides, in the 2010 Haiti earthquake, the intermediate supports of a bridge over Momance River were also damaged by pounding (DesRoches 2011). In the 2008 Wenchuan earthquake also, both Gaoyuan and Miaoziping bridges collapsed due to the breakdown of the shear key after pounding of girders (Han 2009). Such a structural pounding, imposing big flash weight on structure additionally, is very likely to result in initial destruction and deviation (unseating) of the upper structure, and then again, of abutments and piers successively (Robert 1998).

For this reason, there have been many studies on bridge pounding under seismic load. Among them are analytical and theoretical studies on pounding cases, and also preventive ones on the basis of previous analysis and theories. As an analytical type of study on bridge pounding, Han *et al*. (2009) studied the damage that the 2008 Wenchuan earthquake did to a bridge on the highway. Zhang *et al*. (2008) also studied the bridges in California under seismic shaking or liquefaction-induced lateral spreading and found that they were vulnerable to the earthquake to each different degree based on their types. As another type of theoretical study on pounding, Tanabe *et al*. (1998) idealized pounding of upper structures in terms of nonlinear spring, and proved pounding considerably contributed to collapse of an overbridge (a bridge which is continuously pierced on the ground) by performing a time history analysis using the seismic load generated in the 1995 Hyogo-ken Nanbu earthquake. Kajita *et al*. (1998) simulated inter-girder pounding in an element equipped with a linear spring and a damper, and performed a time history analysis to analyze the overbridge response resulted from pounding between adjacent upper structures. On the basis of such analytical and theoretical studies, Robert *et al*. (1998) remarkably analyzed a pounding between upper structures of an elevated isolated bridge, due to the spread of seismic load, and proved by means of numerical simulation that bridge pounding occurred in proportion to the size of gap between upper structures, while emphasizing the fact that too big or too small size of gap could be a problem, too. Shehata (2009) developed a model for an analysis of expansion joint, carrying out a nonlinear time history analysis on an isolated multi-span bridge with three

∗Corresponding author, Research Professor
E-mail: cg-kim@hanmail.net
[a]Professor
[b]Ph.D. Student
[c]Research Professor

ISSN: 1225-4568 (Print), 1598-6217 (Online)

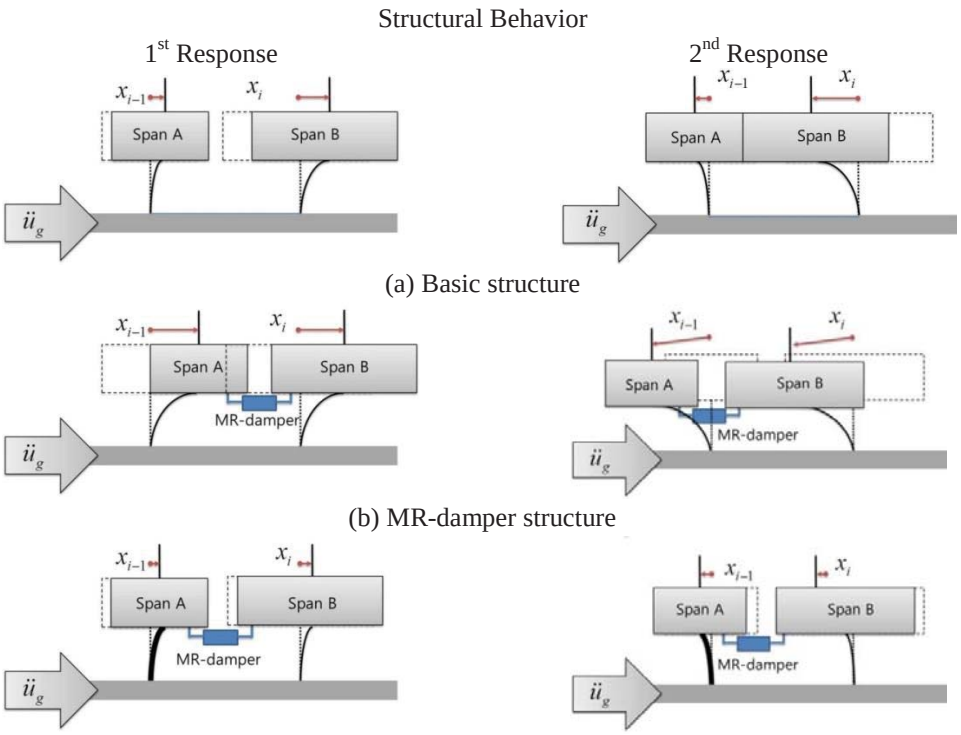

(a) Basic structure

(b) MR-damper structure

(c) HSRC structure

Fig. 1 Concept and expected effect of HSRC system

standard ground motions. Then, he classified the arrangement pattern of restrainer into three types to study which was most effective for pounding mitigation. As a result, he proved the bridge was effectively protected from span unseating and pounding, but failed to protect two upper structures from colliding each other. El-Bahey and Bruneau (2012) in their study attempted to dissipate seismic force by installing a steel damper between a pier and a girder. However, its energy dissipation effect was found limited.

Lately, studies are focused on how to apply MR-dampers to protect the separation layer of existing isolated bridges from pounding due to its increasing displacement. The most representative analytical study of this kind was made by Ruangrassamee *et al*. (2003). After installing four MR-dampers on an analytical model of highway bridge composed of 2 decks (5 spans each), they made an analytical comparison of their performance for response mitigation, using the Kobe seismic load. Li *et al*. (2006) also studied a method to analyze and control the seismic pounding responses of urban elevated bridges (bridges damaged by earthquake-induced pounding). In particular, they tried to control the seismic pounding response of adjacent upper structures using MR-dampers, and theoretically analyzed the performance of the MR-dampers, the one installed at the adjacent upper structure and the other put up between the superstructure and piers. Sheikh *et al*. (2012) studied the effect of MR-damper to damp pounding of a Base-isolated RC Highway Bridge modeled by Matlab & Simulink. However, it was not experimentally verified. The representative experimental study of this kind was made by Guo *et al*. (2009) who connected two MR-dampers to each span and pier installed with rubber bearings for prevention of pounding. Yang *et al*. (2011) studied for a reduction of seismic longitudinal response on suspension bridges by means of the SDOF generalized system that connects the pier and the girder with MR-damper, which was found effective. Li *et al*. (2016) proposed a method that the damage of the bridge can be uniformly distributed throughout the bridge. The pier and girder of three span continuous bridges are connected by MR-damper, and it is proved by simulation. However, in this study, the damage control of the piers only in the extreme earthquakes was made for the study purpose, and the pounding between adjacent girders was not considered.

But it had some disadvantages when the span was connected to the pier, increasing the shear force and moment for supporting piers (Shehata 2009). The previous studies have shown that in order to damp relative displacement of nearby structures under seismic load, it was necessary to place a control device between adjacent upper structures rather than between superstructures (Li 2006, Shehata 2009). However, even when it–happens, that is, a control device is connected to somewhere between adjacent upper structures, the behavior of each upper structure may affect others, increasing the shear force on bearings.

For the reasons, this study proposes a hybrid seismic response control (HSRC) System to control structural behavior under a huge external impact like seismic load, and verifies its performance experimentally. In it, both MR-damper and rubber bearing work together as a unified control system: that is, a MR-damper as a semi-active device that connects upper structures each other, and a rubber bearing as a passive device whose stiffness was

strengthened to resist against increasing shear force caused by application of the MR-damper. In order to verify its performance experimentally, a two upper-span bridge model was built, each span made of different size. Also, three control devices were manufactured: a 10 kN rubber bearing (RB), and another of 20 KN strengthened for this particular purpose, and an MR-damper of 30 KN. Finally, while inflicting El-Centro earthquake load to the structure, its behavior under the load was monitored to verify the HSRC system's control performance. As a result, it was proven effective to mitigate structural behaviors under seismic load.

2. Hybrid Seismic Response Control (HSRC) system

A basic structure of two span bridge without any control devices applied, when it is inflicted with some external load, has a double-degree of freedom. Its 1st and 2nd responses to the load are illustrated in Fig. 1(a). Meanwhile, when an MR-damper is installed for control between upper layers (MR-damper structure) as seen in Fig. 1(b), vibration is controllable to a certain degree, thanks to the different masses of two upper spans as well as to the MR-damper. However, its seat devices get overburdened with too much shear force. It is generally known that when a seismic load is imposed on a bridge laterally, the shear force on bridge seat devices and piers tend to increase (Qin 2012). In this case, it is necessary to effectively minimize both the lateral force affecting piers and the shear force on seat devices. For the purpose, an enhanced rubber bearing (E-RB) was installed on the bridge seat device, thereby completing a HSRC system along with a formerly installed MR-damper. This HSRC system, as seen in Fig. 1(c), is established by integrating a RB, a stiffness-upgraded passive device which was designed to resist the shear force, and also an MR-damper, a semi-active device. It should be also noted that in Fig. 1(c) below, the RB on the left is an enhanced RB (E-RB, 20kN) while the one on the right a general type of 10kN.

2.1 Motion equation of HSRC system

The proposed HSRC system is simplified as seen in Fig. 2. Its relation is also expressed by a general equation of motion as in Eq. (1).

$$\begin{bmatrix} m_i & 0 \\ 0 & m_{i+1} \end{bmatrix} \begin{Bmatrix} \ddot{x}_i \\ \ddot{x}_{i+1} \end{Bmatrix} + \begin{Bmatrix} F_{RB_i} \\ F_{RB_{i+1}} \end{Bmatrix} + \begin{Bmatrix} F_{MR} \\ -F_{MR} \end{Bmatrix} = \begin{bmatrix} m_i & 0 \\ 0 & m_{i+1} \end{bmatrix} \ddot{u}_g \quad (1)$$

Where m is an upper layer mass, and $\ddot{x}$ and $\ddot{u}_g$ indicate an acceleration of the structure and of the ground respectively. In the meantime, a lateral control force generated by RB is expressed by F_{RB}, and F_{MR} is a control force of the MR-damper used for connecting two upper spans. It is generally known that both RBs and MR-dampers under seismic load tend to behave nonlinearly (Ying 2013, Kwok *et al*. 2007). In this study, the Bouc-wen model was adopted particularly to describe the nonlinear behavior of RBs and MR-dampers. It is usually good at describing a non-linear system, first expressed by Bouc (1967) and then further developed by Wen (1976). In addition, it is widely adopted by various fields of study to capture nonlinearity in hysteretic behaviors (Kwok *et al*. 2007, Ikhouane and Dyke 2007, Ikhouane *et al*. 2007). Such hysteric behaviors are modeled using linear stiffness, damping, and hysteretic stiffness, each of which is affected by displacement, velocity, and hysteretic displacement. Hysteretic displacement is calculated as in Eq. (2).

$$\dot{z} = A\dot{x} - \beta\left|\dot{x}\right|z\left|z\right|^{n-1} - \gamma\dot{x}\left|z\right|^{n} \quad (2)$$

Where $\dot{x}$ is velocity, and A, γ, β, and n are fitting parameters. RB restoration force is calculated by the following equation.

$$F_{RB} = k\left(\alpha x + (1-\alpha)z_{RB}\right) \quad (3)$$

Where α is a post-yield stiffness factor and $\alpha \leq 1$. A MR-damper control force can be expressed using the hysteretic displacement on the same principle as in Eq. (4) (Ikhouane and Dyke 2007).

$$F_{MR} = \alpha_{\dot{x}}\dot{x}_{MR} + \alpha_z z_{MR} \quad (4)$$

Where $\dot{x}_{MR}$ and z_{MR} indicate a piston velocity and a hysteretic displacement of the MR-damper respectively, while α_x and α_z damping and hysteretic parameter respectively as defined in Eq. (5).

$$\begin{aligned} \alpha_{\dot{x}} &= \alpha_{\dot{x}1}I + \alpha_{\dot{x}0} \\ \alpha_z &= \alpha_{z1}I + \alpha_{z0} \end{aligned} \quad (5)$$

Where α_{x1} and α_{z1} are active damper constants generated by Current I supplied to the MR-damper, while α_{x0} and α_{z0} are manual damper constants of the manual control force generated by the mechanical performance of the MR-damper.

2.2 Control algorithm

An MR-damper, a kind of semi-active device, performs its function of control only after a control algorithm is applied. In this study, the clipped-optimal control algorithm was adopted for MR-damper. It is a method of designing an optimum linear controller $K_c(S)$, calculating a control force required for MR-damper, and then finally designing MR-damper itself by using the relation between a required

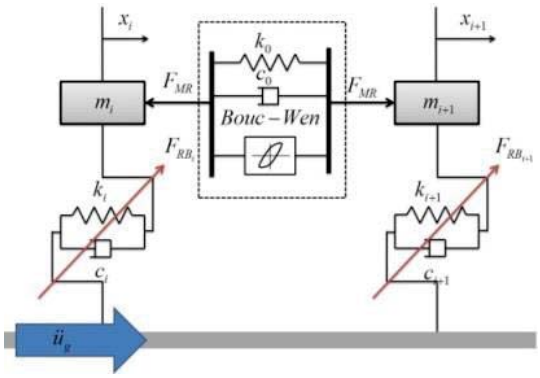

Fig. 2 A Bridge simplified into a 2 DOF system with the HSRC system

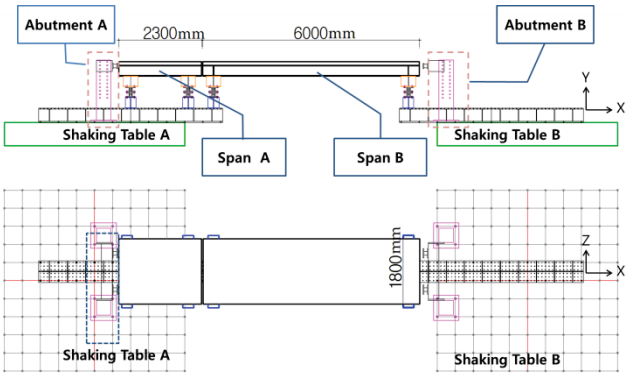

Fig. 3 Configuration and arrangement of two span bridge

control force and a current control force. A required control force is calculated by Eq. (6) on the basis of structural responses.

$$f_c = L\left\{-K_c(s)L\left\{\begin{matrix} y \\ f \end{matrix}\right\}\right\} \tag{6}$$

Where $L\{\cdot\}$ is Laplace transform. To approach a required control force f_c, MR-damper control voltage v_i should be adjusted. Control voltage v_i can be calculated by Eq. (7), and Eq. (7) is a control law of semi active feedback vibration control system where the clipped-optimal control algorithm is applied.

$$v_i = V_{\max} H\left(\{f_{ci} - f_c\} f_i\right) \tag{7}$$

Where v_i is a control voltage that should be input into each controller at the moment, and $V_{\max}$ refers to a max voltage to be flowed in infiltrated at the current stage. In addition, f_{ci} is a required control force of the i^{th} MR-damper, and f_i is a control force observed at the i^{th} MR-damper. When an MR-damper exerts its required control force, it needs to be provided with the control voltage corresponding to a current structural state. It is not until in the case of $f_{ci}=f_i$ that a control voltage signals 0.

2.3 Test structure

A two-span bridge was built with two spans of different size so as to be unsymmetrical in mass as seen in Fig. 3 in order to test the HSRC System's control performance.

The two-span bridge in Fig. 3 is structured to have upper structure, lower structure, and abutment. The upper structure is designed with I type girders to support reinforced concrete slabs. The upper span A is a comparatively short one, 2300mm in length and 1476kg in weight, while the upper span B is a longer one that extends 6000mm long and weighs 3492kg. Both upper spans were designed to be 1800mm in width. RBs, a kind of passive control device, while supporting the upper spans, function as a device for control of structural behavior under seismic load. The lower structure was designed with mini short beams of I type to minimize the structural influence that the piers exert for their stiffness. Also, abutments were installed to protect the upper spans from falling down. The whole structure was placed on the two shaking tables owned by

(a) Experimental setup

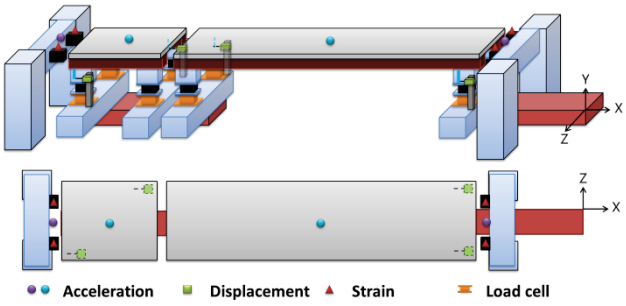

(b) Sensor location

Fig. 4 Experimental setup and sensor location for shaking table test

Table 1 Results of rubber bearing 1 calibration

Span	A	γ	β	n	k (N/mm)	α	ζ
A(RB)	1.253	0.324	0.676	1.000	1359.958	0.649	0.015
B(RB)	2.209	0.992	0.008	1.000	960.017	0.708	0.052

The Seismic Simulation Test Center of Korea as seen in Fig. 4 (a) to perform shaking table tests.

The sensors were placed for the measurement of structural responses; they are an accelerometer, a potentiometer, a load cell, and a strain gage as shown Fig. 4 (b).

3. Hysteretic model of HSRC system

3.1 Hysteretic model of RB

An experiment to calculate RB's hysteretic parameter was performed on the basic structure with RB placed between its upper and lower structure. All RBs adopted for this particular experiment had a capacity of 10 KN. The seismic load was of PGA 0.313 measured at 117 El Centro Array #9 in 1940, but it was value reduced by 70% of its original El Centro for shaking table experiment. From the experiment, load cell data, acceleration, and displacement of upper spans were obtained and then used for calculation of parameters in the Bouc-Wen model. Each value of the parameter is listed in Table 1.

To verify the validity of the RB Bouc-Wen model for correct expression of the RB's nonlinear behavior, the computer simulation was compared with the experiment about the two-span bridge. The following graph in Fig. 5 displays their comparison.

As seen in Fig. 5, the results of simulation where the Bouc-Wen model was applied to express the RB a those of the experiment, which means that the RB Bouc-wen model was excellent at modeling its nonlinear behavior.

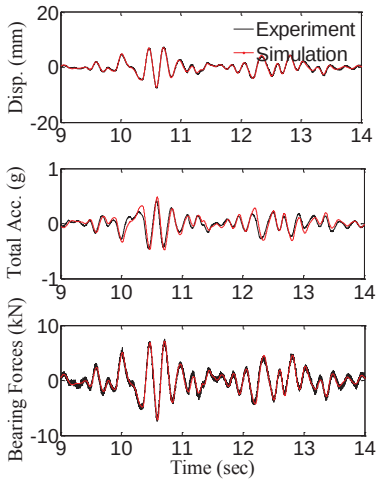

(a) Response data of upper structure A

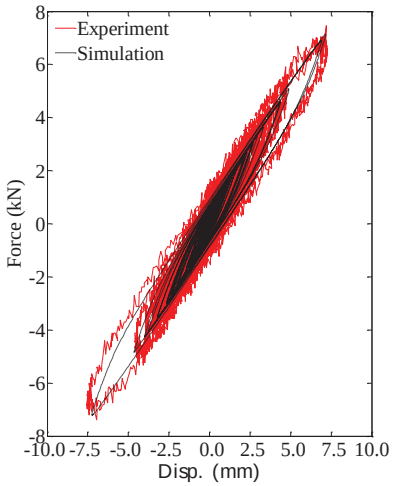

(b) Force-displacement graph of upper structure A RB

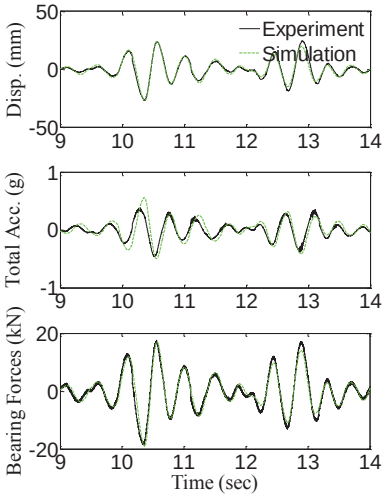

(c) Response data of upper structure B

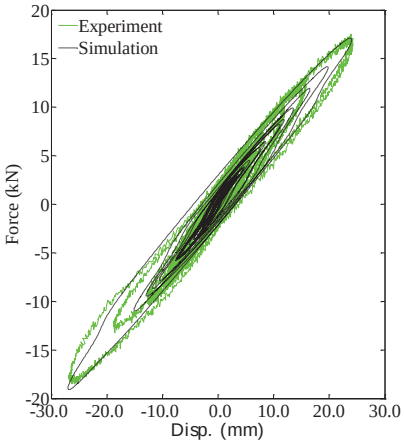

(d) Force-displacement graph upper structure B RB

Fig. 5 Verification of hysteretic model based on test result: RB

Table 2 Results of rubber bearing 2 calibration

Span	A	γ	β	n	k (N/mm)	α	ζ
A(E-RB)	0.751	0.800	0.200	1.000	2401.899	0.589	0.034

Table 3 MR-damper hysteretic model parameters

$\alpha_{\dot{x}1}$ (N.sec/mm.A)	$\alpha_{\dot{x}0}$ (N.sec/mm)	α_{z1} (N /mm.A)	α_{z0} (N /mm)	i_{max} (A)	A_{mr}	γ_{mr}	β_{mr}	n
126.800	64.700	455.700	12.000	3.000	5.585	0.193	0.807	1.000

In order to calculate hysteretic model parameters of E-RB, the RB placed on the upper left span A was replaced by a 20kN RB. In proportion to increased stiffness of RB, a ton of load was additionally inflicted on the span A, while two tons on the span B. Likewise, the El Centro seismic was also increased to 100% from 70% for this experiment. The calculated hysteretic parameters are as follows Table 2.

Since enhanced RBs were applied only to the span A, their hysteretic parameters were also extracted only from it. Again, in order to verify the validity of the Bouc-Wen model applied with the hysteretic parameters in Table 2 for correct expression of their nonlinear behavior, both simulation and experiment result were compared as in Fig. 6 below.

As seen in Fig. 6(a), the simulated graph based on the E-RB Bouc-Wen model very closely matches that of the experiment. Fig. 6(b) also shows that simulation is congruent to experiment in spite of some change in inflicted load on the spans. Therefore, it is verified that the Bouc-Wen model accurately expressed both the RB model and the E-RB model.

3.2 Hysteretic model of MR-damper

For a semi-active control device of the HSRC system, a 30kN MR-damper of SANWA TEKKi corporation was selected because it has been already found effective in controlling the vibration of bridge by the past research. In order to extract hysteretic model parameters of an MR-damper, a test on its performance was taken at the Korea Railroad Research Institute where the damper test equipment was set at 0.4 Hz sin, ±20 mm moving range. For the test, four different currents (0A, 1A, 2A, and 3A)

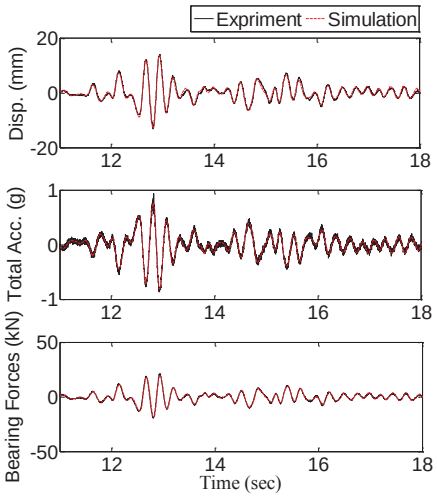

(a) Response data of upper structure A

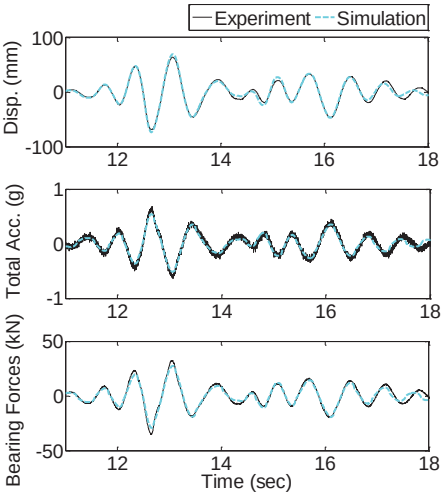

(b) Response data of upper structure B

Fig. 6 Verification of hysteretic model based on test result: E-RB

were supplied to the MR-damper to figure out a relation between supplied current and control force. Among the results acquired from the test, those of the MR-damper's control capacity, displacement and velocity were used to abstract its Bouc-Wen model parameters. Bouc-Wen model parameters of the MR-damper are calculated on the basis of the above results and listed in Table 3.

It is necessary to prove that the Bouc-wen model accurately expresses the MR-damper's nonliteral behavior so that simulation is compared to experiment as in Fig. 7.

Fig. 7 shows a force-displacement graph where the continuous line indicates simulation results while the dotted line those of experiment. As seen in the graph, the simulation, when applied with the MR-damper's Bouc-wen model, is found to closely copy its nonlinear behavior in spite of slight difference which is caused by a failure to take into account installation error while abstracting hysteretic parameters.

3.3 Verification of hysteretic model

Now, it is also necessary to verify whether RB, E-RB, MR-damper's hysteretic parameters would all function properly for the HSRC system so that their simulation was compared to their pre-test results. First, the simulation was done on the basis of the equation of motion (Eq. (1)) where the Bouc-wen model was applied so as to incur a nonlinear behavior of the HSRC system. For a pre-test, the HSRC system was installed into the two span bridge (lumped mass 3 ton), supplying 0A to the MR-damper. Throughout the simulation and the pre-test, 100% of the El Centro seismic load was inflicted. In the graph in Fig. 8, the test results (blue) of the HSRC system's behavior control is compared to the relative displacement between span A and B among the simulation results (red).

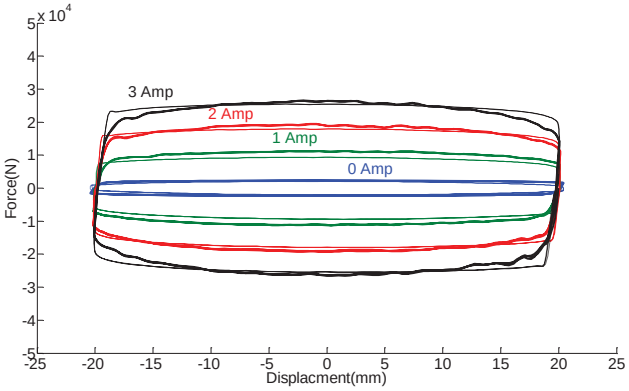

Fig. 7 Verification of hysteretic model based on Bouc-wen model: MR-damper

As seen in Fig. 8, it was observed both results were almost identical even when weight increased. The max error is observed to be 5.4% for RMS relative displacement responses between spans.

4. Shaking table test

Finally, an experiment was carried out to verify a validity of the HSRC system for control of structural behavior. For the experiment, a two-span bridge was placed on two shaking tables (60 ton each, available for the 3 degrees of freedom experiment under the 30-ton payload condition) which were in turn put into operation under the El Centro seismic load. The experiment was performed under the following conditions:

Experimental Cases

Case1. Basic structure condition (Refer to Fig. 1(a))

Case2. MR-damper-applied condition (Refer to Fig. 1(b))

Case3. E-RB-applied condition: RB of span A is replaced with E-RB under the basic structure condition

Case 4. HSRC -applied condition (Refer to Fig. 1 (c))

Case5. HSRC & Clip-applied condition: The clipped-optimal control algorithm is applied to the HSRC system.

As the control flowchart in Fig. 9 shows, the input seismic load was applied to the structure using the shaking table, and the response from the structure was acquired through various sensors. Next, a required control force of the structure was extracted using the linear optimal controller, and a required control force is applied to the

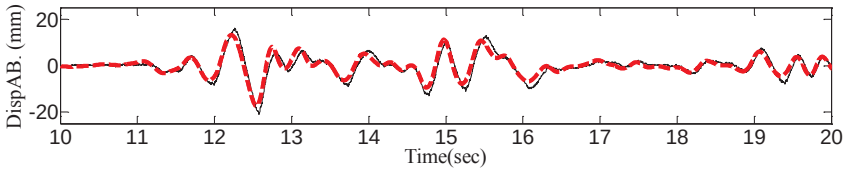

Fig. 8 Verification of simulation result based experimental data: HSRC system

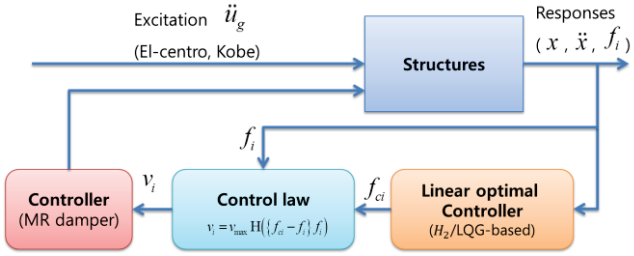

Fig. 9 Control scenario flowchart for performance evaluation of HSRC system

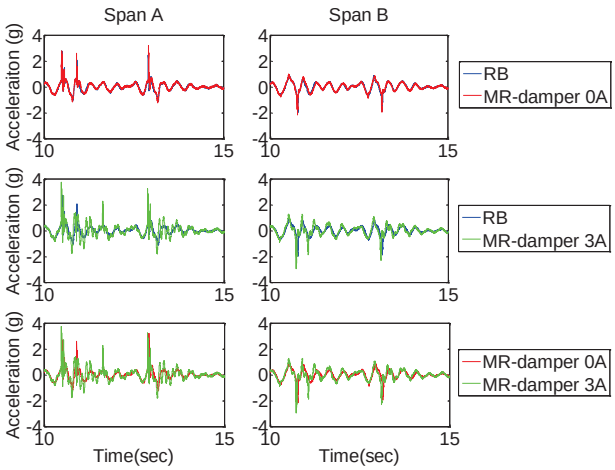

(a) Acceleration

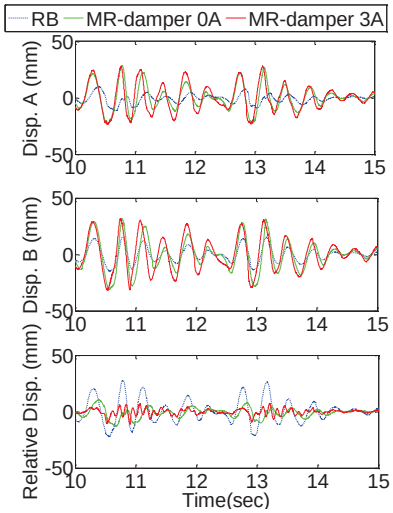

(b) Displacement and relative displacement

Fig. 10 Comparison of test results about case 1 and case 2

control algorithm. Finally, the control signal was supplied to the MR-damper in accordance with the control law.

As an equipment to measure structural responses at various conditions and perform control on the basis of analyzed data, a DS1103 PPC Controller of dSPACE was employed. A PMC 18-3A DC Power Supply of KIKUSUI was also selected as an equipment to flow in electricity to the MR-damper following output voltage from the controller.

4.1 Behavior control test result: Case 1 and 2

In the Case 1, pounding of upper spans is likely to occur under seismic load. To prevent such a pounding from occurring, an MR-damper was attached to the basic structure as in Fig. 1(b) (Case 2), and then an experiment about behavior control was carried out to investigate its role and problem. In it, 130% of El Centro seismic load was excited. The experiment result was compared to the displacement between span A and B, relative displacement between the two spans, and acceleration response data of both spans so as to verify the effect of mitigating earthquake responses under each condition.

As seen in Fig. 10, relative displacement was the most conspicuous at Case 1. Accordingly, it is clear that pounding between two upper spans is most likely to occur under the basic structure condition as shown in Fig. 1(a). As manifested from the acceleration response in Fig. 10(a), it is found that the upper spans often clash with the adjacent abutment. However, when two spans clash with abutment, their behavior energy diminishes, and so two spans themselves did not clash each other.

In the Case 2 as in Fig. 10, relative displacement between two spans was lower than in Case 1 as predicted in Fig. 1(b), but increasing displacement of upper spans also increased impact force between the upper spans and the abutment (a rise of acceleration). In particular, when 3A was supplied to the MR-damper, frequency of pounding increased due to the increase of its control force. As a result, it was found that the MR-damper was able to mitigate relative displacement by connecting two spans. On the other hand, its strong control force made two spans behave as a single structure, thus imposing excessive shear force on the RB.

4.2 Behavior control test result: Case 3 and 4

Shaking table tests for Case 3 and 4 were taken to verify the HSRC system, using 150% of El Centro 150% seismic load. Acceleration, displacement, and relative displacement of spans A and B, obtained from this experiment, are illustrated in Fig. 11 to show the HSRC system was much more effective in behavior control than the MR-damper only applied the condition.

As seen in Fig. 11 the experiment result of Case 3

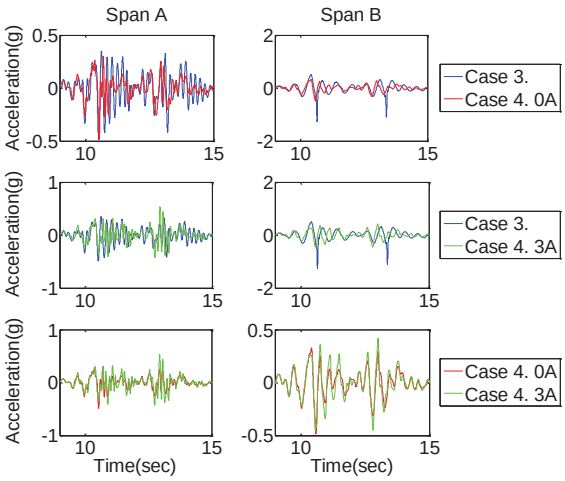

(a) Acceleration

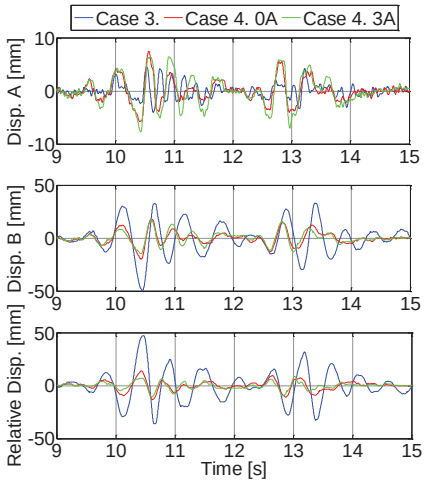

(b) Displacement and relative displacement

Fig. 11 Comparison of test results about case 3 and case 4

showed pounding between span A and abutment was prevented though it was found in Fig. 10(a). However, pounding continued to occur between span B only with a RB of 10 KN and abutment. Since the HSRC system was applied later, no pounding has been observed as seen in Fig. 11(a).

Also, the HSRC system reduced relative displacement between upper spans, and also displacement of span B significantly. As for span A, however, its displacement increased even though RB was replaced by E-RB. Such a phenomenon is caused by span B whose behavior was not completely dispersed by the MR-damper.

The experiment result of case 4, viewed more closely, says displacement of span An increased by around 3 mm at maximum with 0A supplied to the MR-damper, and by around 4 mm also at the maximum, this time, with 3A to the MR-damper. However, in spite of the increased displacement of span A, displacement of span B is reduced by about 30 mm at maximum with 0A supplied to the MR-damper and about 35 mm with 3A added to the MR-damper. In addition, the relative displacement is also reduced by about 33 mm with 0A supplied to the MR-damper and about 38 mm with 3A added to the MR-damper, indicating the

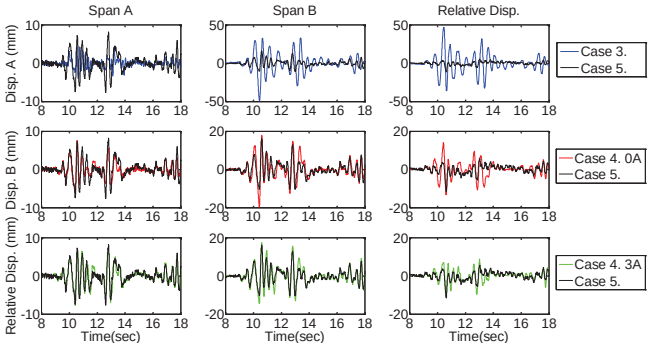

Fig. 12 Comparison of test results about case 3 to 5

increased displacement of span A is almost negligible. Therefore, the experiment proved that hybridization of RB (passive device) and MR-damper MR-damper (semi-active) could perform the best control of structural behavior. In addition, comparing each result supplied either with 0A or with 3A, it is shown that displacement response of span A rather increased at the latter. Such an unexpected phenomenon occurred because the MR-damper exerted more control force than needed for structural response, due to excessive supply of electricity. Consequently, it is necessary to adopt a control algorithm by which control force can be sent to the MR-damper after being adjusted to the bridge structure.

4.3 Behavior control test result: Case 5

Another experiment for the fifth case was performed with a control algorithm applied to the MR-damper of the HSRC system. In Fig. 12, displacement and relative displacement of the upper spans in Case 3 and 4 are compared to those of Case 5.

As seen in Fig. 12, the HSRC System where the clipped-optimal control algorithm is applied was proven more effective for mitigation of displacement and relative displacement of the span B than in Case 3. It also turned out to be effective even when compared to Case 4, especially with 0A supplied to the MR-damper, though a degree of effectiveness may be different. Meanwhile, when compared to the case of 3A supplied to the MR-damper in Case 4, displacement and relative displacement of both spans (A and B) were better mitigated. Table 4 is a quantitative comparison of the values expressed in the graph of Fig. 12 in terms of max value, min value, and RMS value of all data.

As seen in Table 4, in Case 5, i.e. displacement of both spans was reduced more than in Case 4 with 3A current supplied to the MR-damper, and relative displacement was reduced more than 30% compared to Case 4 with no current supplied to the MR-damper. In particular, Case 5 is proven to be more effective for reducing displacement and relative displacement of span B than Case 3. In order to verify the effect of control algorithm applied to the system, Fig. 13 displays acceleration and additional current of both spans, and control force of the MR-damper.

As seen in Fig. 13, the HSRC system where a control algorithm is applied decelerated the upper spans while

Table 4 Comparison of displacement response and relative displacement response (Case 3~5)

	Case 3.			Case 4. 0A			Case 4. 3A			Case 5.		
	Max	Min (-)	RMS	Max	Min (-)	RMS	Max	Min (-)	RMS	Max	Min (-)	RMS
Span A (mm)	4.42	3.97	0.75	7.52	5.72	1.12	6.50	7.70	1.48	8.18	7.65	1.53
Span B (mm)	33.07	49.35	7.66	17.81	19.71	3.10	17.45	14.58	3.03	16.11	10.47	2.59
Relative Disp. (mm)	47.31	36.14	7.61	14.03	13.30	2.27	8.91	11.07	1.71	5.68	11.49	1.51

Table 5 Comparison of control force & additional current of HSRC system for each condition

	Case 4. 0A			Case 4. 3A			Case 5.		
	Max	Min (-)	RMS	Max	Min (-)	RMS	Max	Min (-)	RMS
Force (kN)	8.08	9.90	2.11	11.53	10.70	2.92	8.43	9.76	2.89
Current (A)	0			90003			46218		

reducing current consumption more than in Case 4 with 3A supplied to the MR-damper. In addition, as manifested in the force-displacement graph, the HSRC System was proven to exert an excellent behavior control performance, displaying almost the same amount of control force as in Case 4 with 3A supplied. The result in Fig. 13 can be confirmed from the quantitative result shown in Table 5. Therefore, the HSRC System, where a control algorithm is applied, displayed almost the same amount of control force as in Case with 3A supplied while saving about 50% of electricity.

5. Conclusions

In this paper, the Hybrid Seismic Response Control (HSRC) system was developed to mitigate response of a simple two span bridge under seismic load, and its effectiveness was experimentally verified. For experiments, a two-span simple bridge (bridge model) was manufactured, and the HSRC System was applied to this bridge. Then, the bridge model was mathematically modeled, and its validity was verified through shaking table tests in consideration of the nonlinear hysteretic displacement generated in rubber bearing and MR-damper during experiments.

As the first step of this experiment, a pretest was done to analyze in advance the problems such as span pounding and unseating occurring when rubber bearing only or MR-damper only was used, as discovered in the paper review. Then, three kinds of the experiment were performed to test the HSRC system to prove its effect for mitigation of response under seismic load. The 1st experiment was done at the E-RB state (with E-RB on span A under the basic structure condition), the 2nd one at the HSRC structure state, and the final one at the state with the clipped-optimal control algorithm applied to the HSRC system. Therefore, the following results were obtained.

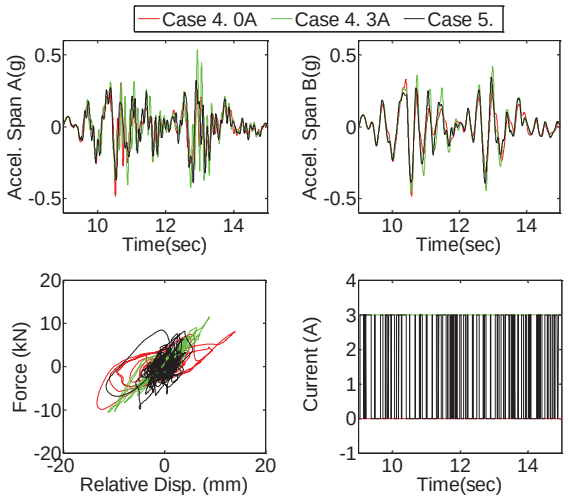

Fig. 13 Comparison of results (HSRC system): Acceleration, control force and current

- When an MR-damper was used to connect two upper spans of bridge, it contributed to a mitigation of relative displacement of spans to a degree (35%, To compared with the case 1 and the case 2(3A)), but it incurred a clash between upper spans and abutment by increasing displacement of spans (Span A 18%, Span B 13%, To compared with the case 1 and the case 2(3A)). That is, in spite of its effectiveness in mitigating relative displacement, the MR-damper, by deforming RB, ended up fixing the upper spans into a single structure and thereby causing pounding.
- When the RB of span A was replaced with the E-RB having a stronger stiffness, pounding between span A and abutment was remarkably mitigated. Later, an MR-damper was additionally placed on the E-RB equipped structure, and then acceleration response of two spans was reduced even in the passive state (Passive on), and both the displacement of span B (60%, To compared with the case 3 and the case 4(3A)) and the relative displacement (78%, To compared with the case 3 and the case 4(3A)) between spans were clearly mitigated. In short, the HSRC system was proven effective of behavior control of adjacent structures.
- When a control algorithm was applied to the HSRC System to add semi-active control, the effect for reducing displacement of span B (15%, To compared with the case 4(3A) and the case 5) and relative displacement (12%, To compared with the case 4(3A) and the case 5) was much stronger than under the passive state of the HSRC system. In summary, the control based on the semi-active performance (with a control algorithm applied) was proven effective while saving energy (48%, To compared with the case 4(3A) and the case 5).

Therefore, the HSRC System was proven to be very effective for behavior control under seismic load, solving the previously addressed problems which resulted from connecting adjacent upper spans by means of control devices.

Acknowledgments

This research was supported by National Research Foundation of Korea through funding from the Ministry of Education (Project No: NRF- 2016R1A2A1A05005499). Many appreciation and acknowledgements go to the National Research Foundation who made this research possible.

References

Bouc, R. (1971), "Modèle mathématique d'hystérésis", *Acustica*, **24**(3), 16-25.

DesRoches, R., Comerio, M., Eberhard, M., Mooney, W. and Rix, G.J. (2011), "Overview of the 2010 Haiti Earthquake", *Earthq. Spectra*, **27**(S1), S1-S21.

Dyke, S.J., Spencer, Jr. B.F., Sain, M.K. and Carlson, J.D. (1996), "Experimental verification of semi-active structural control strategies using acceleration feedback", *Proceeding of 3rd International Conference on Motion and Vibration Control*, **3**, 291-296.

El-Bahey, S. and Bruneau, M. (2012), "Bridge piers with structural fuses and bi-steel columns. I: Exp Test", *J. Bridge Eng*., ASCE, **17**(1), 25-35.

El-Bahey, S. and Bruneau, M. (2012), "Bridge piers with structural fuses and bi-Steel columns. II: analytical investigation", *J. Bridge Eng*., ASCE, **17**(1), 36-46.

Guo, A., Li, Z., Li, H. and Ou, J. (2009), "Experimental and analytical study on pounding reduction of base-isolated highway bridges using MR dampers", *Earthq. Eng. Struct. Dyn.*, **38**, 1307-1333.

Han, Q., Du, X., Liu, J., Li, Z., Li, L. and Zhao, J. (2009), "Seismic damage of highway bridges during the 2008 Wenchuan earthquake", *Earthq. Eng. Eng. Vib*., **8**, 263-273.

Heo, G., Kim, C. and Lee, C. (2013), "Experimental test of asymmetrical cable-stayed bridges using MR-damper for vibration control", *Soil Dyn. Earthq. Eng.*, **57**, 78-85

Heo, G.H. and Jeon, S.G. (2013), "Characteristics and dynamic modeling of MR damper for semi-active vibration control", *J. Korea Inst. Struct. Mainten. Inspect.*, **17**(6), 61-69.

Ikhouane, F. and Dyke, S.J. (2007), "Modeling and identification of a shear mode magnetorheological damper", *Smart Mater. Struct.*, **16**(3), 605-616.

Ikhouane, F., Mañosa, V. and Rodellar, J. (2007), "Dynamic properties of the hysteretic Bouc-Wen model", *Syst. Control Lett.*, **56**(3), 197-205.

Jankowski, R., Wilde, K. and Fujino, Y. (1998), "Pounding of superstructure segments in isolated elevated bridge during earthquakes", *Earthq. Eng. Struct. Dyn.*, **27**(5), 487-502.

Kajita, Y., Sugiura, K., Tsumura, Y., Maruyama, T. and Watanabe, E. (1998), "Numerical Analysis on the Scenario of Girder Fall-off of Simple Span Elevated Bridge during Strong Ground Motions", *Fifth Pacific Structural Steel Conference*, **8**(1), 583-588.

Kwok, N.M., Ha, Q.P., Nguyen, M.T., Li, J. and Samali, B. (2007), "Bouc-Wen model parameter identification for a MR fluid damper using computationally efficient GA", *ISA Tran.*, **46**(2), 167-179.

Lei, Y. and He, M. (2013), "Identification of the nonlinear properties of rubber-bearings in base-isolated buildings with limited seismic response data", *Sci. China Technol. Sci.*, **56**(5), 1224-1231.

Li, Z.X. and Yue, F.Q. (2006), "Analysis and control for seismic pounding responses of urban elevated bridges", *4th International Conference on Earthquake Engineering Taipei*, Paper No. 083.

Li, Z.X., Chen, Y. and Shi, Y.D. (2016), "Seismic damage control of nonlinear continuous reinforced concrete bridges under extreme earthquakes using MR dampers", *Soil Dyn. Earthq. Eng.*, **88**, 386-398.

Qin, H. and Guo, W.D. (2012), "Group effects of piles due to lateral soil movement", *Int. J. GEOMATE*, **4**(1), 450-455.

Raheem, S.E.A. (2009), "Pounding mitigation and unseating prevention at expansion joints of isolated multi-span bridges", *Eng. Struct.*, **31**, 2345-2356.

Ruangrassamee, A. and Kawashima, K. (2003), "Control of nonlinear bridge response with pounding effect by variable dampers", *Eng. Struct.*, **25**, 593-606.

Sheikh, M.N., Xiong, J. and Li, W.H. (2012), "Reduction of seismic pounding effects of base-isolated RC highway bridges using MR damper", *Struct. Eng. Mech.*, **41**(6), 791-803.

Tanabe, T., Machida, A., Higai, T. and Matsumoto, N. (1998), "General view of the reasons for seismic damages for bridge piers and columns of elevated bridges at Hyogoken-Nanbu earthquake", *Structural Engineering World Congres*s, T153-4.

Wen, Y.K. (1976), "Method for random vibration of hysteretic systems", *J. Eng. Mech.*, **102**(2), 249-263.

Yang, M.G., Chen, Z.Q. and Hua, X.G. (2011), "An experimental study on using MR damper to mitigate longitudinal seismic response of a suspension bridge", *Soil Dyn. Earthq. Eng.*, **31**(8), 1171-1181.

Zanardo, G., Hao, H. and Modena, C. (2002), "Seismic response of multi-span simply supported bridges to a spatially varying earthquake ground motion", *Earthq. Eng. Struct. Dyn.*, **31**, 1325-1345.

Zhang, J., Huo, Y., Brandenberg, S.J. and Kashighandi, P. (2008), "Effects of structural characterizations on fragility functions of bridges subject to seismic shaking and lateral spreading", *Earthq. Eng. Eng. Vib.*, **7**(4), 369-382.

CC